Cellular and Molecular Life Sciences

RESEARCH ARTICLE

Developmental regulation of p70 S6 kinase by a G protein-coupled receptor dynamically modelized in primary cells

**Astrid Musnier · Domitille Heitzler · Thomas Boulo ·
Sophie Tesseraud · Guillaume Durand · Charlotte Lécureuil ·
Hervé Guillou · Anne Poupon · Eric Reiter · Pascale Crépieux**

Abstract The mechanisms whereby G protein-coupled receptors (GPCR) activate signalling pathways involved in mRNA translation are ill-defined, in contrast to tyrosine kinase receptors (TKR). We compared a GPCR and a TKR, both endogenously expressed, for their ability to mediate phosphorylation of 70-kDa ribosomal S6 kinase p70S6K in primary rat Sertoli cells at two developmental stages. In proliferating cells stimulated with follicle-stimulating hormone (FSH), active p70S6K was phosphorylated on T389 and T421/S424, through cAMP-dependent kinase (PKA) and phosphatidyl-inositide-3 kinase (PI3K) antagonizing actions. In FSH-stimulated differentiating cells, active p70S6K was phosphorylated solely on T389, PKA and PI3K independently enhancing its activity. At both developmental stages, insulin-induced p70S6K regulation was consistent with reported data. Therefore, TKR and GPCR trigger distinct p70S6K active conformations. p70S6K developmental regulation was formalized in a dynamic mathematical model fitting the data, which led to experimentally inaccessible predictions on p70S6K phosphorylation rate.

Keywords p70S6K · G protein-coupled receptor ·
Dynamic model · Differentiation

A. Musnier · D. Heitzler · T. Boulo · G. Durand · A. Poupon ·
E. Reiter · P. Crépieux (✉)
BIOS Group, INRA, UMR85,
Unité Physiologie de la Reproduction et des Comportements,
37380 Nouzilly, France
e-mail: Pascale.Crepieux@tours.inra.fr

A. Musnier · D. Heitzler · T. Boulo · G. Durand · A. Poupon ·
E. Reiter · P. Crépieux
CNRS, UMR6175, 37380 Nouzilly, France

A. Musnier · D. Heitzler · T. Boulo · G. Durand · A. Poupon ·
E. Reiter · P. Crépieux
Université François Rabelais, 37041 Tours, France

A. Musnier · D. Heitzler · T. Boulo · G. Durand · A. Poupon ·
E. Reiter · P. Crépieux
Haras Nationaux, 37380 Nouzilly, France

S. Tesseraud
INRA UR83 de Recherches Avicoles, 37380 Nouzilly, France

C. Lécureuil · H. Guillou
The Inositide Laboratory, The Babraham Institute,
Cambridge CB2 4AT, UK

Introduction

The 70-kDa ribosomal S6 kinase (p70S6K) is a serine/threonine kinase critically involved in cell growth control in vivo [1, 2]. In vitro, serum-induced entry into S phase of fibroblasts is impaired by anti-p70S6K antibodies [3], indicating a role in cell cycle control. Among other substrates, p70S6K phosphorylates ribosomal S6 protein (rpS6), a component of the 40S eukaryotic ribosomal subunit [4] which plays a role in the ribosome cohesion and in its recruitment to the m7GTP structure of the mRNAs [5]. p70S6K also phosphorylates eukaryotic initiation factor 4B (eIF4B) which enhances the helicase activity of the eukaryotic initiation factor 4A (eIF4A) [6, 7]. Both are part of the pre-initiation translational complex, and their activation induced by p70S6K is thought to enhance translation initiation [8].

In response to growth factors, p70S6K gets phosphorylated [9]. One reference model postulates that the phosphorylation of p70S6K induced by serum or growth factor addition proceeds stepwise [10, 11]. Phosphorylation

of the T421/S424 site located in the autoinhibitory domain relieves the intramolecular inhibition exerted on T389, located in the linker region. T389 is the important residue which, when phosphorylated, serves as an anchoring point to PDK1 (3-phosphoinositide-dependent kinase) whose substrate, among others, is the T229 located in p70S6K activation loop [12, 13]. All those inducible phosphorylation events depend on the phosphoinositide-3 kinase (PI3K)/mammalian target of rapamycin (mTOR) pathway and, accordingly, are inhibited by the PI3K inhibitor LY294002 and the mTOR inhibitor rapamycin [12]. The complexity of the PI3K/mTOR pathway is incremented with feedback loops and cross-talks with other pathways, such as the MAP kinase-dependent signaling, which are mainly integrated at the level of TSC2 [14, 15].

It is commonly admitted that p70S6K is conformationally active only once those three sites at least have been phosphorylated. However, data suggesting that this particular sequence of p70S6K phosphorylation may be functionally uncoupled from p70S6K enzymatic activity now lead to stem from this view. For example, mutations in the carboxyterminal end of p70S6K indicate that these phosphorylation sites are not involved in controlling enzyme activity in mitogen-stimulated 3T3 fibroblasts [16]. Even more, in mitotic cells, paclitaxel, a chemotherapeutic agent which destabilizes microtubules, has been shown to stimulate phosphorylation of p70S6K on T421/S424, concurrently with catalytic inactivation of the enzyme [17], indicating that phosphorylation of this region of p70S6K may even be linked to enzyme inactivation. In addition, in response to G protein-coupled receptors (GPCR), agonists recognizing the thyroid-stimulating hormone receptor [18], the prostaglandin F2α receptor [19], the endothelin receptor [20], or the α1-adrenergic receptor [21] respectively, epistatic elements such as PI3K may not be activated [18, 19], or may even be inhibited [21], despite activation of p70S6K.

Our own results in differentiating primary Sertoli cells stimulated by follicle-stimulating hormone (FSH) also contradict the commonly admitted model of p70S6K regulation [22]. FSH importance in mammalian reproduction has long been acknowledged and has been confirmed both in male and in female, by knocking out the FSH receptor (FSH-R) [23] or the specific FSHβ subunit [24]. At the cellular level, FSH controls the proliferation and differentiation of somatic cells of the gonads: granulosa cells of the ovarian follicle and Sertoli cells of the seminiferous tubules [25, 26]. Those stages are separate during the testis development: Sertoli cells proliferate perinatally and proceed through their differentiation program until the end of puberty.

The FSH-R is a GPCR whose coupling to heterotrimeric protein Gs and to scaffolding proteins, namely β-arrestins

[27], accounts for most FSH cellular responses. Gs coupling leads to protein kinase A (PKA) activation, which phosphorylates several nuclear as well as cytosolic targets. In primary differentiating Sertoli cells, our group has previously shown that FSH enhances p70S6K catalytic activity via PKA activation, which is also responsible for the dephosphorylation of the T421/S424 residues. PI3K was not involved in the regulation of this site [22], and was not stimulated by FSH in these cells. Nevertheless, PI3K dynamically maintained a constitutive level of T389 phosphorylation, required for further p70S6K activation in response to FSH. Of note, insulin stimulation of these cells led to inducible phosphorylation of both the T421/S424 and T389 residues, consistently with the current model of stepwise phosphorylation of p70S6K in response to growth factors as mentioned above [10].

All these observations outline the complexity of p70S6K regulation and address the following question: is the particular activation of p70S6K that we have observed in differentiating Sertoli cells, a hallmark of GPCRs such as the FSH-R, or is it dependent on the cell developmental stage, i.e., does it vary in proliferating versus terminally differentiating Sertoli cells? To address this question, we sought to analyze and to dynamically model the p70S6K activation pathways in proliferating primary Sertoli cells isolated from 5-day-old rats and stimulated with FSH or with insulin.

Materials and methods

Materials

Human FSH was purchased from Merck Serono (Geneva, Switzerland) and insulin from Sigma Chemical (St Louis, MO). Porcine FSH was purified by Dr Jean Closset (Université de Liège, Belgium). LY294002 and rapamycin were purchased from Cell Signaling Technology (Beverly, MA) and Myr-PKI from Calbiochem (San Diego, CA). Antibodies raised against phospho-p70S6K [T389], phospho-p70S6K [T421/S424], phospho-rpS6 [S235/Ser236], phospho-mTOR [S2448], phospho-Foxo1 [S256], rpS6, and Foxo1 were purchased from Cell Signaling Technology. Antibodies to ERK1, 2, to mTOR and to p70S6K were purchased from Santa Cruz Biotechnology (Santa Cruz, CA). Horseradish-coupled peroxidase antibody was purchased from GE Healthcare UK (Buckinghamshire, UK). Cholera toxin (CTX) was from Sigma Chemical.

Primary Sertoli cell culture

Animals were treated following the current ethical guidelines of the European Community. Sertoli cells were

isolated from testes of 5- or 19-day-old Wistar rats and seeded in DMEM (InVitrogen Life Technologies, Carlsbad, CA) complemented (DMEMc) with penicillin (100 IU/ml), streptomycin (100 μg/ml), glutamine (2 mM), retinol (50 ng/ml), vitamin E (200 ng/ml), and human transferrin (5 μg/ml), all purchased from Sigma Chemical, as reported previously [28]. At 24–48 h after purification, cells were exposed to the PI3K inhibitor LY294002 (50 μM, 10 min) or to the mTOR inhibitor rapamycin (10 nM, 60 min), or to the PKA inhibitor Myr-PKI (50 μM, 60 min), or were left untreated before being exposed to human FSH (100 ng/ml) or to human insulin (100 ng/ml) from 5 to 60 min, or to cholera toxin for 60 min. To minimize non-specific effects, dose-responses of the various pharmacological inhibitors were carried out. The experiments were performed with the minimal efficient concentrations of pharmacological inhibitors that did not affect cell viability, determined by a MTT assay, as described [29]. The results presented herein show the response at 60 min for the p70S6K activity and hormone stimulation alone and at 30 min for hormone stimulation following pharmacological treatment.

p70S6K activity assay

The activity of the enzyme was measured by quantifying the incorporation of γ-^{33}P-ATP on 11 amino-acids of S6 sequence (^{229}AKRRRLSSLRA^{239}) according to the manufacturer's instructions (Upstate Cell Signaling, Lake Placid, NY), as described previously [22].

Western blot analysis

Cells were lysed in p70S6K activity lysis buffer as described above, and 20 μg of proteins were separated by SDS-PAGE and transferred to nitrocellulose membrane (Whatman, Dassel, Germany). Membranes were saturated with TBST-BSA (Tris Buffer Saline with 0.1% Tween 20, 3% Bovine Serum Albumin) and were probed with rabbit primary antibodies (1:1000): anti-phospho-p70S6K1 [T421/S424], anti phospho-p70S6K1 [T389], anti-phospho-rpS6 [S235/Ser236] or anti-phospho-mTOR [S2448]. Membranes were also probed to detect the total corresponding protein, and reprobed with an anti-ERK1, 2 antibody to monitor gel loading. Western blots were revealed with Supersignal West Pico Chemiluminescent Substrate or Supersignal Femto Chemiluminescent Substrate from Pierce Biotechnology (Rockford, IL). Films were scanned and the optical density of the signals was measured with ImageMaster 1D Elite version 4 software (Amersham Biosciences).

Phosphatidyl-inositide (3, 4, 5) trisphosphate assay by protein-lipid overlay

To estimate PI3K activity, PIP3 was quantified in Sertoli cells as described recently [30]. Briefly, PtdIns-rich fractions were extracted with chloroform/methanol, selectively isolated on neomycin beads, eluted with methanol–choloroform–HCl. Purified PtdIns were spotted onto a nitrocellulose membrane, blotted overnight at 4°C with the PH domain of the general receptor for phosphoinositide 1 (GRP1) fused to GFP. Membranes were then probed with a rabbit anti-GFP polyclonal antibody coupled to HRP, the chemiluminescence was detected with the ECL reagent (Amersham) and acquired with the Image Reader LAS-1000 charge-coupled device (CCD) camera (Fujifilm). Densitometry was measured with the AIDA software with local background subtraction.

cAMP quantification by ELISA

One million Sertoli cells was seeded in 24-well plates and stimulated with increasing doses of FSH ranging from 10 to 400 ng/ml, during 15 min, or with 100 ng/ml FSH in a time-course ranging from 5 to 120 min. The experiments have been performed in the presence of 100 μM phosphodiesterase inhibitor IBMX (isobutyl-methylxanthine; Sigma Chemicals). Results were expressed in percent of the response to 10 μM of the adenylate cyclase activator Forskolin (Sigma Chemicals) for 15 min in the dose-response experiments or for 60 min for the time-course experiments. cAMP was measured directly in the cell media using a competition assay, according to the manufacturer's instructions (Biomedical Technologies, Stoughton, MA).

Binding assays and Scatchard analysis

One million Sertoli cells stimulated with porcine FSH was plated in poly-lysine-coated 24-well plates. Binding assays were performed the next day, essentially as described in [27]. Both the number of cells and the global protein content were found as equivalent in the two cell types, at the end of the experiment. The affinity constant was calculated from the binding data using Scatchard analysis.

Mathematical model

A single model of the regulation of p70S6K was built and parameterized in differentiating and proliferating cells. The differences that were observed experimentally in some reactions between the two stages were expressed by considering two reactions, one being catalyzed, and one being

spontaneous. In the cell stage where the considered reaction was catalyzed, the parameter corresponding to the spontaneous reaction was null and, conversely, in the cell stage where the reaction was spontaneous, the parameter corresponding to the catalyzed reaction was null. The model can be represented by a non-linear system of 13 ODEs (ordinary differential equations, see below) with 24 unknown parameters (Table 1), corresponding to kinetic rates and total amounts of the different molecules involved.

Parameters were estimated as follows: the amount of FSH was considered as constant throughout the 60 min of experiment, regardless its capture by the FSH-R. In addition, we considered that no FSH receptor was lost during the experiment. Consequently, the total quantity of receptors (R_T), which is the quantity of free receptors (R) plus the quantity of receptors complexed with the hormone (RH), was considered as constant (see conservation law CL1). Similarly, the total amount of nucleoside A_T (ATP and cAMP), of phosphatidyl-inositol P_T (PIP2 and PIP3), of p70S6K S_T (non-phosphorylated p70S6K and the three different phosphorylated forms) and rpS6: $rpS6_T$ (phosphorylated PrpS6 and non-phosphorylated rpS6) were considered as constant, as further supported by our experimental data for p70S6K and rpS6. This can be formalized by the following 5 conservation laws, which leads to removing 5 ODEs:

Table 1 Parameters, constants, and variables in the dynamic model of p70S6K regulation by FSH

Definition	Name in ODEs	Value in proliferating cells (5 dpp)	Value in differentiating cells (19 dpp)
Receptor binding association rate	$k1$	0.01 μg/nmol/s	
Activation of cAMP PKA pathway	$k2$	0.7 μg/nmol/s	
Activation of PI3K PIP mTOR pathway	$k3$	5 μg/nmol/s	0.25 μg/nmol/s
Desactivation of cAMP PKA pathway	$k4$	0.025 μg/nmol/s	
Phosphorylation rate (S6KP1 → S6KP1P2)	$k5$	0.1 μg/nmol/s	0.00001 μg/nmol/s
Phosphorylation rate (S6KP2 → S6KP1P2)	$k6$	0.001 μg/nmol/s	
Phosphorylation rate (S6K → S6KP1)	$k7$	0.018 μg/nmol/s	0.00001 μg/nmol/s
Phosphorylation rate (S6K → S6KP2)	$k8$	0.0001 μg/nmol/s	
Dephosphorylation rate (S6KP1P2 → S6KP1)	$k9$	0.1 μg/nmol/s	
Dephosphorylation rate (S6KP2 → S6K)	$k10$	7 μg/nmol/s	
Dephosphorylation rate (S6KP1P2 → S6KP2)	$k11$	0.02/s	
Dephosphorylation rate (S6KP1 → S6K)	$k12$	0.000001/s	
Phosphorylation rate (rpS6 → PrpS6)	$k13$	4 μg/nmol/s	
Total amount of FSH	$k14$	5.58 nmol/μg	
Total amount of receptor	$k15$	0.0558 nmol/μg	0.0744 nmol/μg
Total amount of ATP	$k16$	1 nmol/μg	4.37 nmol/μg
Total amount of PIP	$k17$	0.5 nmol/μg	0.75 nmol/μg
Total amount of p70S6K	$k18$	0.4 nmol/μg	4 nmol/μg
Total amount of rpS6	$k19$	0.8 nmol/μg	
1% cAMP value	$k20$	0.00336 (10^6 cells)/μg	0.00263 (10^6 cells)/μg
1% insulin value	$k21$	0.0005 (10^6 cells)/μg	
Dephosphorylation rate (PrpS6 → rpS6)	$k22$	0.22/s	0.18/s
Receptor affinity constant	Kd_RH	10.64664 nmol/μg	6.88344 nmol/μg
PIP2 ↔ PIP3 reaction constant ($k23/k3$)	Kd_PIP	0.1407 nmol/μg	13.420304 nmol/μg
Dephosphorylation rate (S6KP2 → S6K) at equilibrium	$k10/k8$	70,000	
Phosphorylation rate (S6KP2 → S6KP1P2) at equilibrium	$k6/k11$	0.05	
Dephosphorylation rate (S6KP1P2 → S6KP1) at equilibrium	$k9/k5$	1	10,000
Phosphorylation rate (S6K → S6KP1) at equilibrium	$k7/k12$	18,000	10

Common parameters to both stages are indicated for 5 dpp only. At both stages, for insulin $k9$ and $k10 = 0.00001$, hence $k9/k5 = 0.0001$ and $k10/k8 = 0.1$

p70S6K[T389] is noted by S6KP1, p70S6K[T421/S424] is noted S6KP2 and p70S6K[T389/T421/S424] is noted S6KP1P2

s^{-1} corresponds to the time needed by S6KP1P2 to be converted to S6KP2 in 1 μg protein

$$R_T = R + RH \tag{CL1}$$

$$A_T = ATP + cAMP \tag{CL2}$$

$$P_T = PIP2 + PIP3 \tag{CL3}$$

$$S_T = p70S6K + Pp70S6K[T389]$$
$$+ Pp70S6K[T421/S424]$$
$$+ Pp70S6K[T389/T421/S424] \tag{CL4}$$

$$rpS6_T = rpS6 + PrpS6[S235/236] \tag{CL5}$$

The quantities of R, ATP, PIP2, p70S6K and rpS6 can then be computed from the differential equations given below. For the sake of clarity, null quantities where removed from the equations when relevant, leading to two expressions of the same ODE at the two stages: parameters corresponding to a unique reaction with different regulations at the two stages (catalyzed or spontaneous) are noted p (for proliferation stage) and d (for differentiation stage).

For both stages:

$$dRH/dt = k1 \cdot R \cdot H_T - k1 \cdot Kd_{RH} \cdot RH \tag{ODE1}$$

$$dcAMP/dt = k2 \cdot ATP \cdot RH - k4 \cdot cAMP \tag{ODE2}$$

For the proliferation stage:

$$dPIP3/dt = k3p \cdot PIP2 \cdot RH - k3p \cdot Kd_{PIP} \cdot PIP3 \tag{ODE3p}$$

$$dPp70S6K[T389]/dt = k7p \cdot PIP3 \cdot p70S6K$$
$$+ k9 \cdot cAMP \cdot Pp70S6K[T389/T421/S424]$$
$$- k5p \cdot PIP3 \cdot Pp70S6K[T389] - k12 \cdot Pp70S6K[T389] \tag{ODE4p}$$

$$dPp70S6K[T421/S424]/dt$$
$$= k8p \cdot PIP3 \cdot p70S6K + k11 \cdot Pp70S6K[T389/T421/S424]$$
$$- k6.PIP3 \cdot Pp70S6K[T421/S424]$$
$$- k10 \cdot cAMP \cdot Pp70S6K[T421/S424] \tag{ODE5p}$$

$$dPp70S6K[T389/T421/S424]/dt$$
$$= k5p \cdot PIP3 \cdot Pp70S6K[T389]$$
$$+ k6 \cdot PIP3 \cdot Pp70S6K[T421/S424] \tag{ODE6p}$$
$$- k9 \cdot cAMP \cdot Pp70S6K[T389/T421/S424]$$
$$- k11 \cdot Pp70S6K[T389/T421/S424]$$

$$drpS6[S235/236]/dt$$
$$= k13p \cdot rpS6 \cdot Pp70S6K[T389/T421/S424] \tag{ODE7p}$$
$$- k22 \cdot PrpS6[S235/236]$$

For the differentiation stage:

$$dPIP3/dt = k3d \cdot PIP2 - k3d \cdot Kd_{PIP} \cdot PIP3 \tag{ODE3d}$$

$$dPp70S6K[T389]/dt = k7d \cdot PIP3 \cdot p70S6K$$
$$+ k9 \cdot cAMP \cdot Pp70S6K[T389/T421/S424]$$
$$- k5d \cdot Pp70S6K[T389] - k12 \cdot Pp70S6K[T389] \tag{ODE4d}$$

$$dPp70S6K[T421/S424]/dt$$
$$= k8d \cdot p70S6K + k11 \cdot Pp70S6K[T389/T421S424]$$
$$- k6.PIP3 \cdot Pp70S6K[T421/S424]$$
$$- k10 \cdot cAMP \cdot Pp70S6K[T421/S424] \tag{ODE5d}$$

$$dPp70S6K[T389/T421/S424]/dt$$
$$= k5d \cdot Pp70S6K[T389]$$
$$+ k6 \cdot PIP3 \cdot Pp70S6K[T421/S424] \tag{ODE6d}$$
$$- k9 \cdot cAMP \cdot Pp70S6K[T389/T421/S424]$$
$$- k11 \cdot Pp70S6K[T389/T421/S424]$$

$$drpS6[S235/236]/dt = k13d \cdot rpS6 \cdot Pp70S6K[T389]$$
$$- k22 \cdot PrpS6[S235/236] \tag{ODE7d}$$

Data and units

Quantities were expressed in nmol/μg of proteins, as deduced from the experimental data presented herein, or as % of the response to insulin, arbitrarily fixed at 5×10^{-7} mol/g in proliferating cells and at 10^{-6} mol/g in differentiating cells, based on a previous PIP3 quantification in CHO cells [31]. The quantities measured experimentally were PIP3, cAMP, and PrpS6, which correspond to a single node in the model, p70S6K phosphorylated on Thr389, and p70S6K phosphorylated on T421/S424. p70S6K phosphorylated on Thr389 is in fact the sum of Pp70S6K[T389] plus Pp70S6K[T389/T421/S424], while the amount of p70S6K phosphorylated on T421/S424 is the sum of Pp70S6K[T421/S424] and Pp70S6K[T389/T421/S424].

Program, software, fitting algorithm

The ODE model was simulated with the SCILAB software (http://www.scilab.org). Parameter values were adjusted by analyzing the data back and forth with the conjugate gradient method implemented in datafit intern Scilab procedure. The minimized normalized error is the distance between the data and the corresponding quantity simulated in the model.

The p70S6K developmental regulation by FSH has been graphically represented with the CellDesigner graphic interface (http://celldesigner.org).

Statistics

Measurements were performed in duplicates or triplicates and results were expressed as mean values $\pm$ SEM of at least 3 independent experiments. Statistical analysis of the biological data was performed using one-way ANOVA (Bonferroni's multiple comparison tests) to compare samples or two-way ANOVA to compare entire curves (GraphPad PRISM Software, San Diego, CA). Values with $P < 0.05$ were considered as significantly different.

Results

FSH or insulin stimulates p70 S6 kinase enzymatic activity and alters its phosphorylation pattern in primary Sertoli cells from 5 day-old rats

We first sought to determine whether FSH stimulated the activity of p70S6K in proliferating Sertoli cells from 5 day-old rats, as it does in differentiating Sertoli cells from 19 day-old rats [22]. After 1 h of exposure to FSH, p70S6K enzymatic activity increased slightly but significantly (Fig. 1a). Consistently, the phosphorylation of rpS6 also increased after 60 min of FSH stimulation, as shown by western blot analysis (Fig. 1b, c), confirming that p70S6K was activated by FSH. Likewise, both p70S6K activity and rpS6 phosphorylation were stimulated by insulin.

Then, we analyzed p70S6K pattern of phosphorylation on T389 and T421/S424, both sites supposedly required for p70S6K activation [10]. The T421/S424 site was dephosphorylated following FSH stimulation, whereas it was phosphorylated in response to insulin (Fig. 1d, e). In contrast to differentiating Sertoli cells, in proliferating Sertoli cells, T389 phosphorylation was enhanced by FSH (Fig. 1f, g) in a dose-responsive manner (Fig. 1h). However, the level of T389 phosphorylation in response to FSH was lower than the one observed in response to insulin (Fig. 1g).

The hormone-bound FSH-R generates PIP3 and cAMP with a different efficacy in 5 and 19 day-old rat primary Sertoli cells

One characteristic feature of GPCRs when compared to tyrosine kinase receptors is their ability to couple to G proteins. Our previous data suggest that the FSH-R differentially couples to both Gs and Gi in proliferating Sertoli cells and only to Gs in differentiating Sertoli cells [32]. Therefore, we hypothesized that the FSH-R activation might induce the production of second messengers such as cAMP and PIP3 with different efficacy in proliferating and
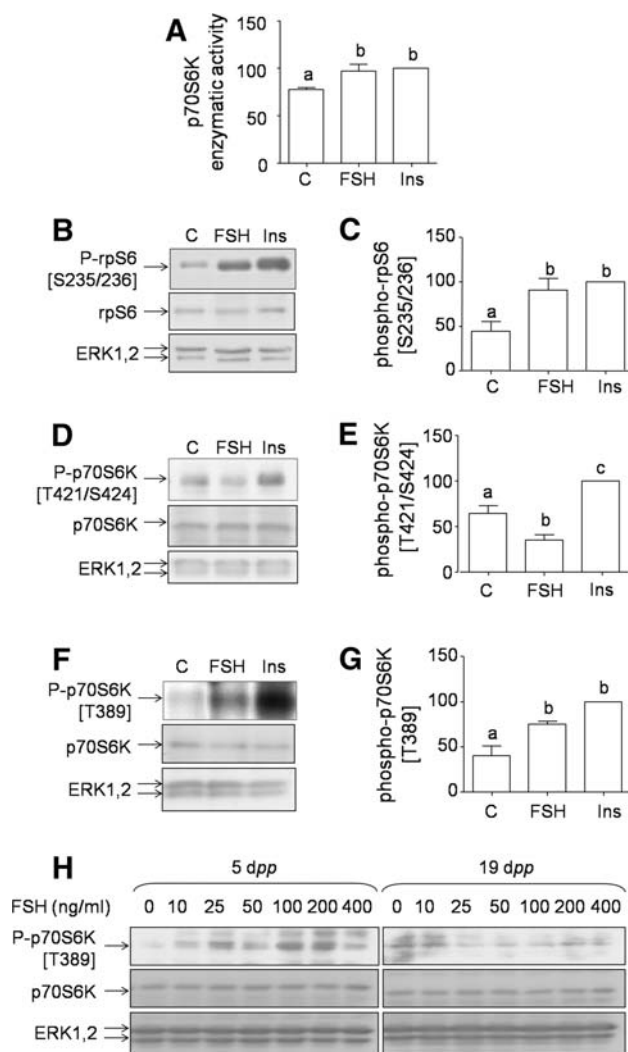
Fig. 1 p70S6K is activated by FSH and by insulin in 5-day-old rat primary Sertoli cells. Sertoli cells were treated for 60 min with 100 ng/ml of FSH or insulin (Ins) or were left untreated C. **a** Mean $\pm$ SEM of p70S6K activity obtained at least from 3 independent experiments each performed in triplicates. **b** Representative western blot of rpS6 phosphorylation on S235/236, reprobed with an anti-total-rpS6 antibody. **c** Mean $\pm$ SEM of rpS6 phosphorylation obtained from more than 3 independent experiments each performed in duplicates. **d, f** Representative western blots of p70S6K phosphorylation on T421/S424 and T389 residues, respectively, reprobed with an anti-total-p70S6K antibody. **h** Representative western blot of p70S6K phosphorylation on T389 induced by increasing doses of FSH in proliferating Sertoli cells (5 d*pp*) and in differentiating Sertoli cells (19 d*pp*) reprobed with an anti-total-p70S6K antibody. In **b, d, f, h**, gel loading was monitored by reprobing the membranes with an anti-ERK1, 2 antibody. **e, g** Means $\pm$ SEM of phospho-T421/S424 and phospho-T389 signals respectively, obtained from 3 independent experiments each performed in duplicates. All the results were expressed as percent of the response to insulin. Shared *superscripts* indicate no significant difference, while different *superscripts* indicate significant differences, at the $P < 0.05$ level

in differentiating Sertoli cells, to account for the developmental differences in signaling to p70S6K. To compare cAMP and PIP3 production at the two developmental

stages, we first had to make sure that second messenger production was measured at similar receptor density in both cell types. By binding assays performed with ^{125}I-pFSH, the displacement curves obtained with proliferating as well as differentiating Sertoli cells matched (Fig. 2a). The Kd values were in similar range, i.e., 5.7×10^{-9} M and 4×10^{-9} M in Sertoli cells from 5- and 19-day-old rats, respectively, as inferred from Scatchard plot analysis (Fig. 2b, c). These results show that the affinity of FSH for its receptor and the receptor density do not vary significantly in both developmental stages (0.04 vs 0.03×10^{-9} M, respectively), in agreement with previous
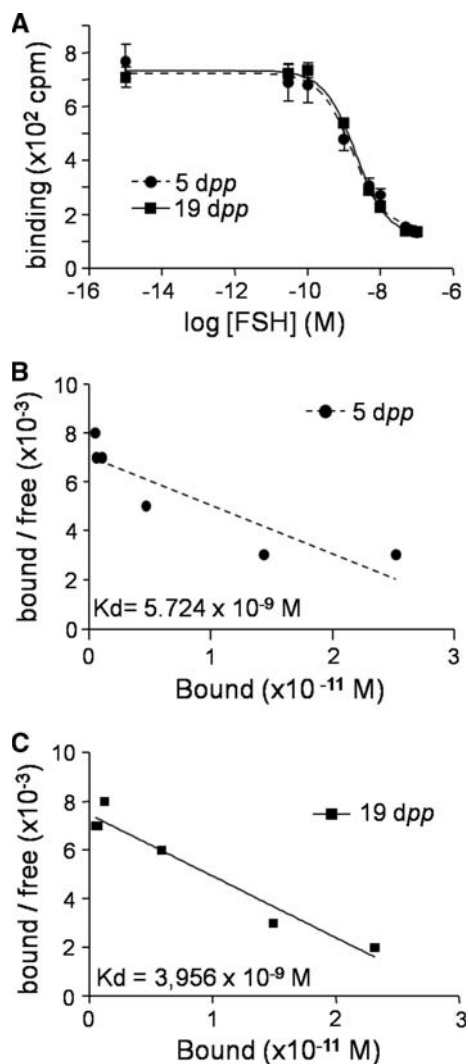

Fig. 2 Comparison of the binding properties of the FSH-R in proliferating and in differentiating Sertoli cells. Binding parameters were estimated in proliferating (*circles*) and differentiating (*squares*) Sertoli cells incubated for 1 h at 37°C in the presence of ^{125}I-pFSH and increasing concentrations of unlabeled pFSH (10^{-14} to 10^{-7} M). Triplicates were done for each concentration of pFSH. **a** The displacement curve represents the mean of three different experiments ± SEM. **b,c** The affinity constant was calculated from the binding data using Scatchard analysis

data obtained from testis homogenates [33]. Thereof, second messenger production can be directly compared.

We previously reported that only in differentiating Sertoli cells did FSH cause a time-dependent increase in cAMP levels, whereas in proliferating cells, cAMP was constitutively elevated, similarly to the cAMP maximum levels reached in FSH-stimulated Sertoli cells from prepubertal rats [32]. Since phosphodiesterases are expressed at much higher levels in differentiating Sertoli cells [34], a phosphodiesterase inhibitor, IBMX, was added to cell cultures 15 min prior to FSH stimulation, in order to compare cAMP production in both cellular backgrounds more accurately. Clearly, the efficacy of FSH to produce cAMP was much higher in differentiating than in proliferating Sertoli cells, as can be observed in time-course (Fig. 3a) as well as in FSH dose-response experiments (Fig. 3b). Forskolin stimulation led to comparable cAMP production in both cell types (4.5 ± 0.53 and 3.79 ± 0.19 pmoles/10^6 cells in proliferating and in differentiating Sertoli cells, respectively; data not shown). Hence, it was considered as an internal control, so that cAMP production could be directly compared at both stages.

Then, PIP3 production was directly quantified by a protein-lipid overlay. In 5-day-old rat cells, PIP3 was significantly increased by FSH stimulation whereas it was not in 19-day-old rat cells (Fig. 3c). This observation suggests an FSH-dependent activation of PI3K in proliferating cells and is consistent with PI3K constitutive activation in differentiating cells. To estimate the efficacy of FSH to produce PIP3, we first assayed whether phosphorylation of the phosphoinositide-dependent transcription factor Foxo1 would correlate to our data. Time-course stimulation with FSH indicated that Foxo1 gets inducibly phosphorylated in proliferating Sertoli cells, whereas it was constitutively phosphorylated in differentiating Sertoli cells (Fig. 3d). Since this result was concordant with the PIP3 direct quantification, the efficacy of FSH to stimulate PIP3-dependent events was next estimated by assaying Foxo1 phosphorylation in dose-response experiments. As expected, we found that increasing doses of FSH nicely enhanced Foxo1 phosphorylation in proliferating cells, but not in differentiating cells where Foxo1 phosphorylation was constitutively high, and could not be further enhanced by FSH (Fig. 3e). Although insulin stimulation for 15 min did not lead to a significant increase in PIP3 production, it enhanced Foxo1 phosphorylation after 1 h. Therefore, PI3K activity is constitutive in differentiating cells, and still can be activated further at both stages by insulin, but only in proliferating Sertoli cells by FSH. In conclusion, the efficacy of the FSH-R coupling to cAMP was more efficient in differentiating Sertoli cells, whereas PIP3-generating mechanisms were more potent in proliferating Sertoli cells stimulated by FSH.
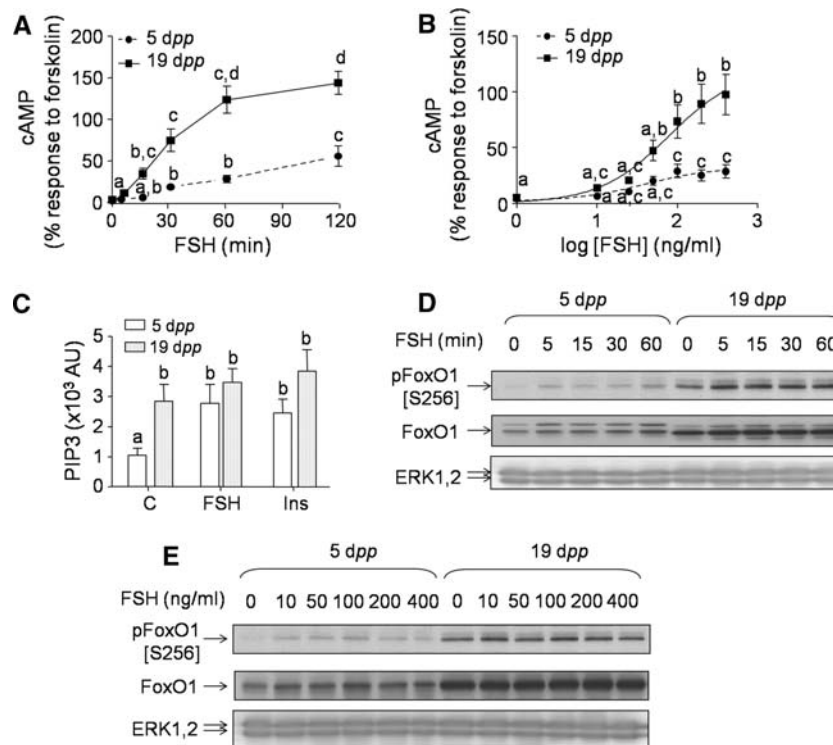
Fig. 3 Developmental regulation of FSH efficacy to induce second messenger production. **a** Mean ± SEM of cAMP production obtained from 3 independent experiments each performed in triplicate, as a function of FSH stimulation time, in proliferating or in differentiating Sertoli cells as indicated. **b** Mean ± SEM of cAMP production obtained from 3 independent experiments each performed in triplicate, as a function of FSH concentration, in proliferating or in differentiating Sertoli cells as indicated. Results are expressed as % of the forskolin-induced cAMP response, taken as an internal control. **c** Sertoli cells isolated from 5 or 19 day-old rats were stimulated with FSH for 15 min or were left untreated. Results shown are the mean values ± SEM of PIP3 production, expressed in arbitrary units (AU)

obtained from more than 3 independent fat ligand blot experiments. **d** Representative western blot of Foxo1 phosphorylation on S256 as a function of FSH stimulation time, in proliferating (5 dpp) or in differentiating Sertoli cells (19 dpp). **e** Representative western blot of Foxo1 phosphorylation as a function of FSH concentration, in proliferating or in differentiating Sertoli cells (19 dpp) reprobed with an anti-total-Foxo1 antibody. In **d** and **e**, gel loading was monitored by reprobing the membranes with an anti-ERK1, 2 antibody. Shared *superscripts* indicate no significant difference, while different *superscripts* indicate significant differences, at the $P < 0.05$ level

Dynamic mathematical simulation of p70S6K regulation by FSH in control conditions

To gain a clearer view of the active forms of p70S6K in response to FSH in the development of Sertoli cells, we achieved dynamic mathematical modelling. All the molecular species studied here were listed as follows: the FSH receptor, the hormone, the hormone-receptor complex, PI3K, activated PI3K, PIP2, PIP3, mTOR, activated mTOR, ATP, cAMP, PKA, the cAMP-PKA complex, rpS6, PrpS6, p70S6K, Pp70S6K[T389], Pp70S6K[T421/S424], and Pp70S6K[T389/T421/S424]. Table 1 lists all the parameters determined in this study, in proliferating and in differentiating Sertoli cells. Quantification of the molecular species and Kd values have been determined as explained in "Materials and Methods". Parameters such as $k3$ and $k5$ vary, as expected from modification of the model structure: for $k3$, PIP3 is no longer increased in differentiating cells. As for k5, the p70S6K regulation is uncoupled

to the PIP3-dependent component in differentiated Sertoli cells.

In our model, we have four different forms for p70S6K: the non-phosphorylated form, two mono-phosphorylated forms (either T389 or T421/S424) and the form with both sites phosphorylated. Consequently, there are 12 possible transitions. Among those, four were eliminated: the double phosphorylation, direct and reverse, and the transitions between the two mono-phosphorylated forms, because dephosphorylation on the T421/S424 site requires FSH stimulation, whereas the dephosphorylation on the T389 site is spontaneous. Consequently, none of these four transitions can be made in a single step, and are in fact the sum of two of the retained transitions.

Since this study focuses on p70S6K regulation nodes, parts of the model were simplified. Based on previous data obtained in differentiating Sertoli cells where inhibiting PI3K or mTOR led to similar consequences on p70S6K regulation [22], the model was reduced by aggregating the

PI3K/PIP/mTOR cascade in a single reaction, considered as a black box: transformation of PIP2 (inactive) in PIP3 (active). Again, on the basis of our previous report [22], the same was done for the cAMP/PKA pathway, also considered as one reaction: the formation of cAMP from ATP.

From experimental data, regulations of four of the reactions were differently regulated in both stages. For example, in differentiating cells, PIP3 reached its steady state in the absence of hormone, and the reaction could be considered as spontaneous. Thereof, the regulation of the conversion rate of PIP2 to PIP3 upon FSH binding was not taken into account for this stage, and only the spontaneous reaction was considered. In contrast, FSH binding to the FSH-R enhanced PIP3 level in proliferating cells and the model indicates that this PIP3 amount was produced more slowly due to low hormone-receptor complex formation. At this cell stage, the parameter representing the spontaneous conversion rate of PIP2 to PIP3 was considered as null.

We obtained two dynamic simulations of the model based on optimized parameters, which fitted the biological data obtained at both stages (Fig. 4). Of note, all but one kinetic parameters corresponding to reactions having the same regulation in both stages are equal (Table 1). This shows that the differences in regulations, formalized as differences in parameters, in initial conditions and total amounts are sufficient to explain the observed differences in p70S6K regulation.

The model provided the intrinsic concentrations of Pp70S6K[T389], Pp70S6K[T421/S424], and Pp70S6K[T389/T421/S424], which are not experimentally observable (Fig. 5a, b). At both stages, Pp70S6K[T421/S424] was initially the major form, to be transformed into p70S6K, Pp70S6K[T389/T421/S424] and indirectly into Pp70S6K[T389]. Whereas the clearance of Pp70S6K [T421/S424] was fast, the evolution of Pp70S6K[T389/T421/S424] and Pp70S6K[T389] remained slower and sustained. When considering Pp70S6K[T389/T421/S424], it remained constant only in proliferating cells, where an increase in Pp70S6K[T389] compensated the decrease in Pp70S6K[T421/S424].

FSH modulates PI3K and mTOR-dependent phosphorylation of p70S6K T389 and T421/S424 residues

To unravel the relationships linking the PI3K/mTOR pathway to p70S6K activation, we analyzed the effect of their inhibition on the p70S6K phosphorylation pattern. LY294002, a PI3K inhibitor, and rapamycin, an mTOR inhibitor, abolished the basal phosphorylation of the T421/S424 site (Fig. 6a, b). Hence, the FSH-induced dephosphorylation was not visible any more. Similarly,
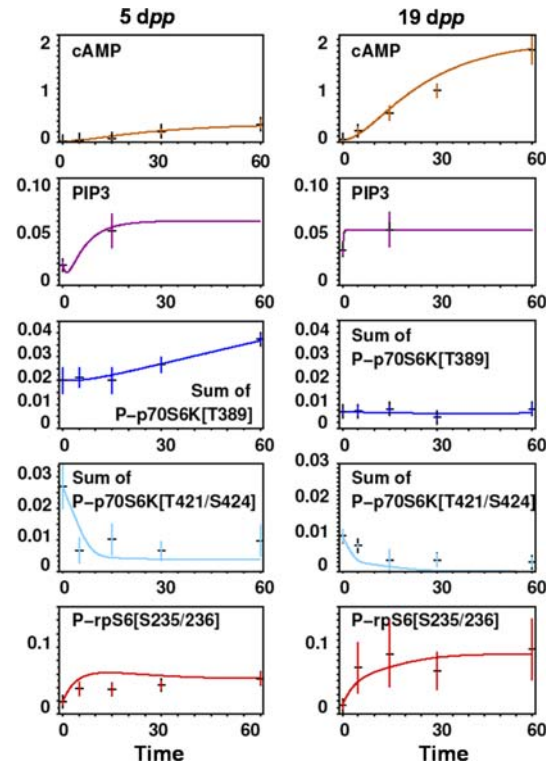

Fig. 4 Simulation of FSH-induced p70S6K regulation. Computational simulations (plain lines) compared with experimental data (black crosses ± SEM) of FSH-R-mediated signaling in proliferating (left) and differentiating (right) Sertoli cells. The concentration of molecules in mmol/g is expressed as a function of time in minutes. "cAMP" stands for the aggregate cAMP-PKA module, "PIP3" stands for the aggregate PI3K/PIP3/mTOR module

both LY294002 and rapamycin considerably reduced basal and FSH-induced T389 phosphorylation (Fig. 6c, d). Therefore, the PI3K-mTOR pathway seems to be involved in the basal phosphorylation of both sites and in the FSH-inducible phosphorylation of T389. As expected, LY294002 and rapamycin inhibited insulin-stimulated phosphorylation of both T421/S424 and T389 sites.

To define whether the PI3K-mTOR pathway impacted on p70S6K activity, we measured rpS6 phosphorylation following cell pre-treatment with LY294002 or with rapamycin. Those inhibitors strongly decreased the phosphorylation of rpS6, which reveals inhibition of p70S6K activity, in response to FSH, and even more to insulin (Fig. 6e, f).

Consistent with the involvement of PI3K and mTOR in FSH-dependent signaling, FSH stimulated mTOR phosphorylation, in a PI3K-dependent manner (Fig. 6g, h). Surprisingly, mTOR was more potently activated by FSH-dependent signaling than by insulin-dependent signaling. However, mTOR phosphorylation was more sensitive to PI3K inhibitors in cells stimulated by insulin than following FSH stimulation, suggesting that other upstream events,
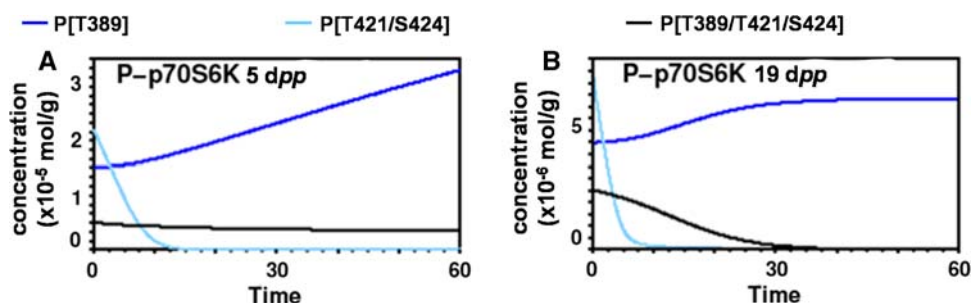
Fig. 5 Intrinsic Pp70S6K quantities predicted by computational simulations, respectively, Pp70S6K phosphorylated on [T389] only, Pp70S6K phosphorylated on [T421/S424] only, and Pp70S6K phosphorylated on [T389/T421/S424], as indicated. Simulations in **a** proliferating and **b** differentiating Sertoli cells are shown
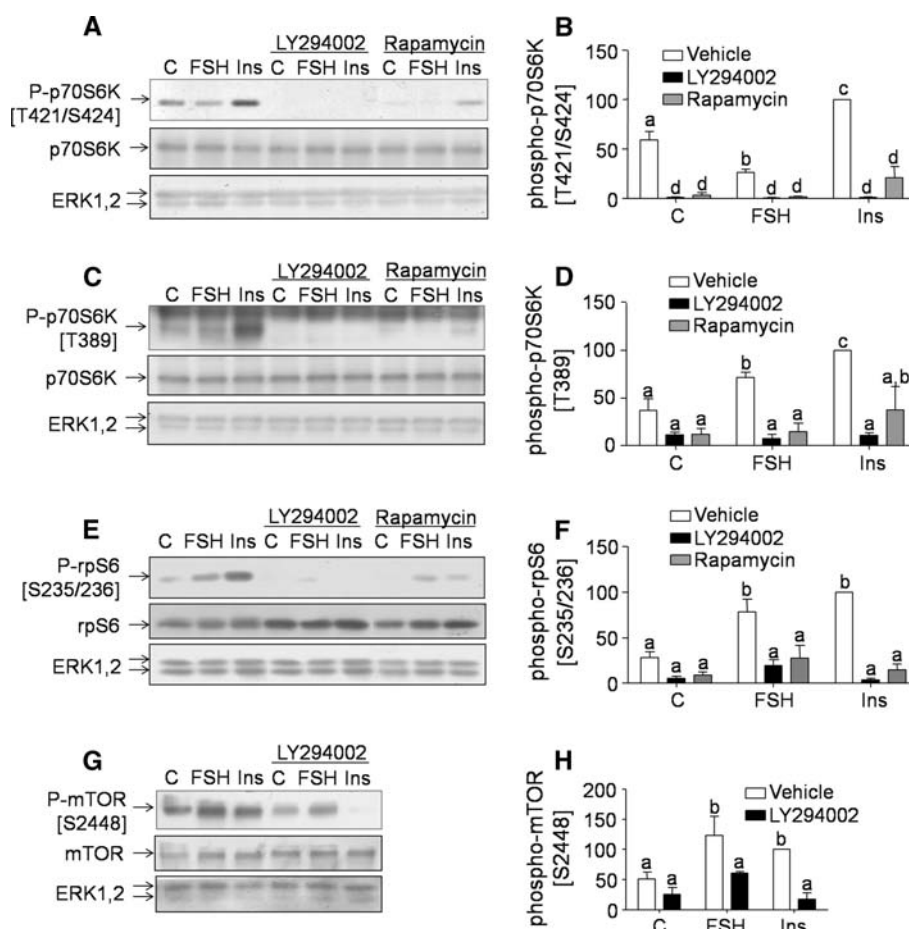

Fig. 6 FSH enhances PI3K and mTOR-dependent phosphorylation of p70S6K T389 and decreases PI3K and mTOR-dependent tonic phosphorylation of T421/S424. Sertoli cells were pretreated with the PI3K inhibitor LY294002 (50 mM, 10 min) or with the mTOR inhibitor rapamycin (10 nM, 60 min) or were left untreated before being stimulated for 30 min with FSH or insulin. **a,c** Representative western blots of p70S6K phosphorylation on T421/S424 and T389 residues, respectively, reprobed with an anti-total-p70S6K antibody. **b,d** Mean ± SEM of phospho-T421/S424 and phospho-T389 signals respectively, each obtained from 3 independent experiments performed in duplicates. **e** Representative western blot of rpS6 phosphorylation on S235/236 reprobed with an anti-total-rpS6 antibody. **f** Mean ± SEM of phospho-rpS6 signals obtained from 3 independent experiments each performed in duplicates. **g** Representative western blot of mTOR phosphorylation on S2448 reprobed with an anti-total-mTOR antibody. In **a**, **c**, **e**, and **g**, gel loading was monitored by reprobing the membranes with an anti-ERK1, 2 antibody. **h** Mean ± SEM of phospho-mTOR signals obtained from 3 independent experiments each performed in duplicates. Results are expressed as percent of the response to insulin. Shared *superscripts* indicate no significant difference, while different *superscripts* indicate significant differences, at the $P < 0.05$ level

unrelated to PI3K, are required for FSH to stimulate mTOR.

We kept the same sets of parameters as for the control conditions to simulate pharmacological perturbations, except for the total amounts of those molecules that were affected by the treatment, namely PI3K and mTOR, which were not represented in our models. In both cases, the consequence of the inhibition of these molecules was a drastic decrease of the available amount of the active form, equivalent to a drastic decrease in the amount of the aggregate variable PIP3, which was modeled by reducing 10-fold the initial and total PIP3 amounts at both stages (Table 1 and Fig. 7). The simulation confirmed that in active PI3K-depleted conditions, Pp70S6K[T389] decreased at both stages, and that Pp70S6K[T421/S424] also decreased in proliferating cells (Fig. 8a, b, to be compared with the simulation in control conditions in Fig. 5a, b). In proliferating cells, loss of Pp70S6K[T389/T421/S424] was concomitant to the loss of rpS6 phosphorylation, while in differentiating cells, only the loss of Pp70S6K[T389] was seen.

Importantly, the fact that our model still fits the observations in perturbed conditions (Fig. 7) without modifying
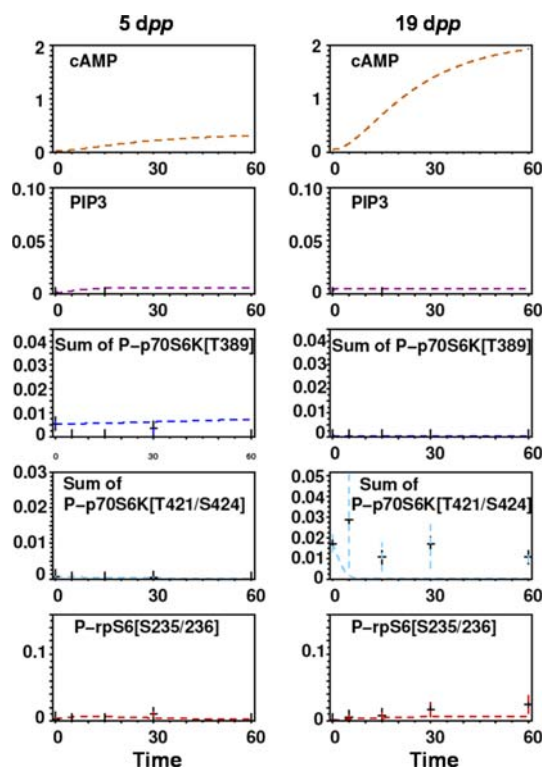
Fig. 7 Simulation of the PI3K/PIP3 component of FSH-induced p70S6K regulation. Computational simulations (*plain lines*) compared with experimental data (*black crosses* ± SEM) of FSH-R-mediated signaling in the presence of PI3K inhibitor, in proliferating (*left*) and differentiating (*right*) Sertoli cells. The concentrations of molecules are expressed as a function of time, as above

the parameters that were obtained in normal conditions (Table 1), further confirms its validity.

p70S6K activation is constitutively restrained by PKA in proliferating Sertoli cells

PKA stimulates p70S6K activity by dephosphorylating the T421/S424 site in differentiating Sertoli cells [22]. Since FSH stimulation also led to dephosphorylation of these residues in proliferating Sertoli cells, we sought to define the role of PKA in these cells. The enzymatic activity of p70S6K was measured in proliferating Sertoli cells pretreated with the PKA highly specific inhibitor, Myr-PKI [35]. Contrasting with differentiating cells, at this stage of development, inhibition of PKA over-stimulated p70S6K activity, which indicates that PKA would have an inhibitory effect on p70S6K (Fig. 9a). These data were further confirmed by western blot analysis, which showed a great increase in rpS6 phosphorylation in similar experimental conditions (Fig. 9b, c).

Since PKA antagonistically acted on p70S6K activity depending on Sertoli cell developmental stage, it was interesting to explore the impact of PKA inhibition on p70S6K phosphorylation pattern in proliferating cells. By western blot analysis, we observed that cell exposure to increasing doses of Myr-PKI led to a gradual raise in phosphorylation of the T421/S424 site (Fig. 9d). This increase was observed in basal as well as in FSH- or insulin-induced conditions (Fig. 9d, e). Similar results were obtained when using a structurally unrelated PKA inhibitor, C-MIQ (data not shown). Conversely, activating Gαs, known to stimulate PKA, by increasing doses of cholera toxin mimicked FSH-induced dephosphorylation of the T421/S424 site (Fig. 9f). In contrast, the T389 site appeared to be insensitive to regulation by PKA (Fig. 9g, h).

As above, PKA, which is the target of Myr-PKI, is not represented in the simplified model. The direct consequence of PKA impairment is a drastic decrease of the available amount of active PKA, equivalent to a drastic decrease of the aggregate variable cAMP. This was modeled in both cell types by dividing initial and total amounts of cAMP 50-fold (Table 1). The simulation in PKA-depleted conditions revealed a large amount of Pp70S6K[T421/S424] at both stages (Fig. 11a, b, to be compared with the simulation in control conditions in Fig. 5a, b), leading to the hypothesis that cAMP indirectly catalyses the dephosphorylation of Pp70S6K[T421/S424]. In addition, in proliferating cells, Pp70S6K[T389] was restrained by PKA depletion. Therefore, at both stages, the PKA pathway indirectly catalyses the transition of Pp70S6K[T389/T421/S424] to Pp70S6K[T389]. The major difference between both stages is that this transition is
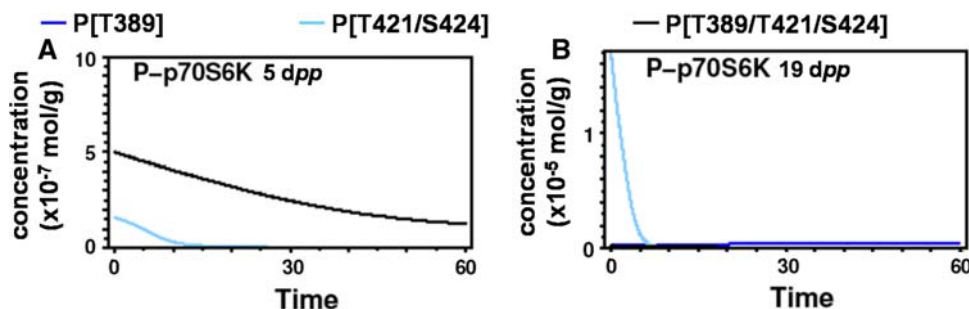
Fig. 8 Intrinsic Pp70S6K quantities predicted by computational simulations, in PI3K-perturbed conditions. As above, the respective levels of Pp70S6K phosphorylated on [T389] only, Pp70S6K phosphorylated on [T421/S424] only and Pp70S6K phosphorylated on [T389/T421/S424], are compared. Simulations in **a** proliferating and **b** differentiating Sertoli cells are shown

inhibitory of rpS6 phosphorylation in proliferating cells, and stimulatory in differentiating cells, as can be inferred from rpS6 phosphorylation level. This is due to the fact that the active form of p70S6K is different at the two stages. We can conclude from these simulations (Fig. 10) that the difference in initial conditions and total amount of the aggregate variable cAMP, figuring the inhibition of PKA, is sufficient to explain the evolution of the phosphorylated forms of p70S6K levels in FSH-stimulated conditions (Fig. 11).

Graphic formalization of p70S6K regulation by FSH

To formalize the differences in p70S6K regulation by FSH accurately, we graphically represented the signaling mechanisms engaged at both developmental stages by using the CellDesigner graphic interface (Fig. 12). It should be noted that in these diagrams, the PKA and mTOR pathways are figured, although they have been aggregated in the model used for simulation. When focusing on p70S6K phosphorylations, it appeared clearly that in proliferating Sertoli cells, only p70S6K phosphorylated on both T421/S424 and T389 was active, regardless the hormone, i.e. FSH (Fig. 12a) or insulin (Fig. 12b). Therefore, we propose that the major difference between FSH versus insulin-induced p70S6K activation is that p70S6K is refrained by the PKA signaling component emanating from FSH stimulation. In contrast, in differentiating Sertoli cells, only p70S6K phosphorylated on T389 is the active form, and PKA relieves the inhibition mediated by constitutive phosphorylation of T421/S424. Insulin-induced phosphorylation of p70S6K was similar at both stages.

Discussion

Here, we demonstrate that FSH-induced p70S6K activation pattern varies as a function of the Sertoli cell developmental stage. In proliferating Sertoli cells isolated from 5-day-old rats, FSH weakly activates p70S6K, and induces dephosphorylation of its T421/S424 site and phosphorylation of its T389 site. FSH-induced T421/S424 dephosphorylation relies on PKA activation, and is detrimental to p70S6K enzymatic activity. The PI3K/mTOR pathway counteracts this inhibitory effect, and is also amenable for FSH-induced T389 phosphorylation. In striking contrast, in differentiating Sertoli cells stimulated by FSH, PKA-induced dephosphorylation of the T421/S424 site is required for its enzymatic activity, and p70S6K is not inducibly phosphorylated on T389 [22]. Tonic activation of the PI3K pathway is important for FSH to activate p70S6K in these cells. Resting concentrations of PIP3 have been shown previously to contribute permissively to carbachol-induced S6K1 activation mediated by the Gq-coupled M3 muscarinic receptor [36].

Importantly, in proliferating as well as in differentiating Sertoli cells treated with insulin, p70S6K pattern of phosphorylation was similar and was consistent with the current model, describing the enzyme as getting fully activated through sequential phosphorylation on multiple sites, including T421/S424 and T389 [10]. Therefore, our results clearly indicate that various patterns of phosphorylation are able to confer an active conformation to p70S6K. More precisely, extracellular signal-induced phosphorylation of the T421/S424 is supposed to relieve p70S6K auto-inhibition. This happens to be the case in proliferating Sertoli cells, but not in differentiating Sertoli cells, which suggests additional mechanisms to support this auto-inhibitory role. Furthermore, one important advance provided by our data is that p70S6K pattern of phosphorylation could be dictated by the class of receptor engaged, i.e., via a tyrosine-kinase receptor for the insulin receptor *versus* a GPCR for the FSH-R.

Here, we proposed a dynamical model of FSH-regulated p70S6K in primary Sertoli cells. The structure of the model was hypothesized from the experiment, and the parameters
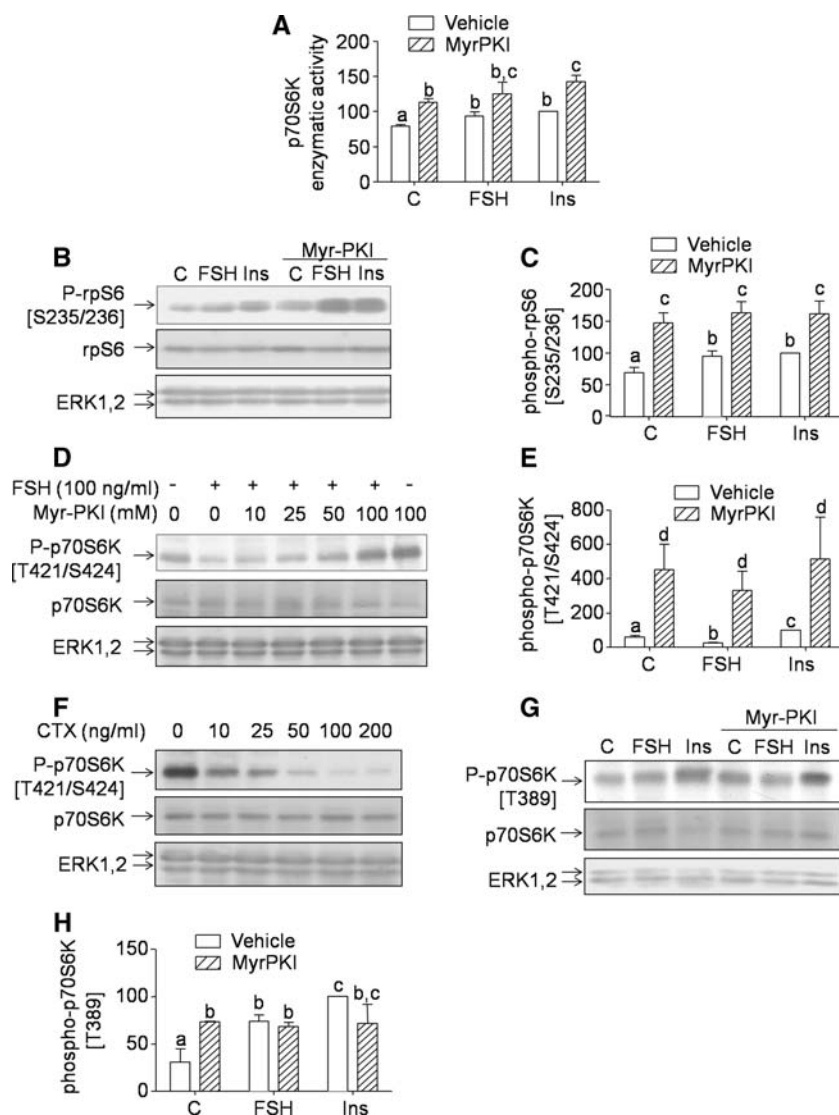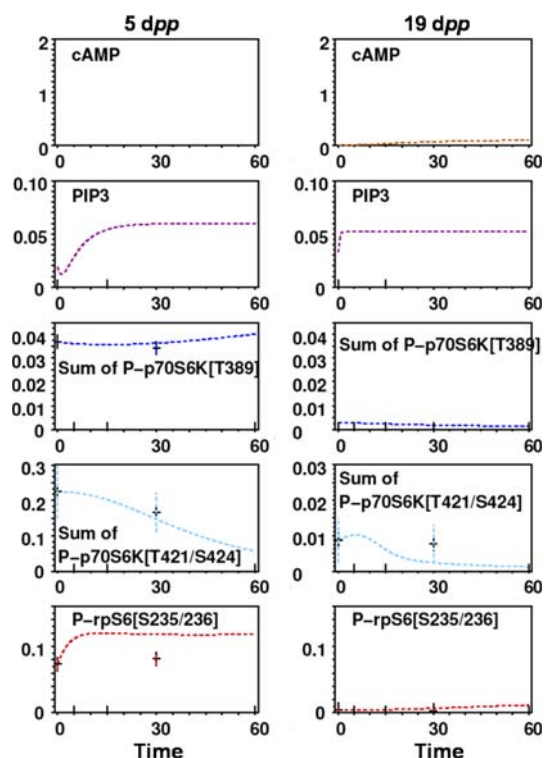
Fig. 9 FSH-induced p70S6K activation includes a PKA-dependent inhibitory component. Sertoli cells were pretreated with the PKA inhibitor Myr-PKI (50 nM, 1 h) or left untreated before stimulation with FSH or insulin (each at 100 ng/ml) for 1 h to measure p70S6K activity or for 30 min for western blot assay. **a** Mean ± SEM of p70S6K activity obtained from 3 independent experiments each performed in triplicates. **b** Representative western blot of rpS6 phosphorylation reprobed with an anti-total-rpS6 antibody. **c** Mean ± SEM of phospho-rpS6 signals obtained from more than 3 independent experiments each performed in duplicates. **d, f** Representative western blots of p70S6K phosphorylation on T421/S424 in response to FSH, in cells incubated with increasing doses of Myr-PKI or CTX, respectively. The membrane was reprobed with an anti-total-p70S6K antibody. **g** Representative western blot of T389 phosphorylation in response to FSH, reprobed with an anti-total-p70S6K antibody. In **b**, **d**, **f**, and **g**, gel loading was monitored by reprobing the membranes with an anti-ERK1, 2 antibody. **e**, **h** Mean ± SEM of phospho-T421/S424 and T389 signals obtained from 3 independent experiments each performed in duplicates. Results are expressed as percent of the response to insulin. Shared *superscripts* indicate no significant difference, while different *superscripts* indicate significant differences, at the $P < 0.05$ level

where optimized to fit data in normal conditions. Although we cannot rule out that this is not the unique solution, we found it satisfactory to obtain a set of parameters which fit the data, given the number of readouts, i.e., cAMP, PIP3, sum of Pp70S6K[T389], sum of Pp70S6K[T421/S424], PrpS6[S235/236], Kd_{RH}, FSH-R, FSH. Therefore, the probability that our parameters are close to reality is enhanced. Our model is further supported by the fact that, although it was obtained by fitting the control conditions, all the parameters, i.e., kinetic rates and total amounts, still fitted the data in pharmacologically perturbed conditions.

Considering the phosphorylated p70S6K isoforms, our model predicts that, in differentiating cells, FSH stimulation increases the level of Pp70S6K[T389], which is ultimately the active form, at the expense of Pp70S6K[T389/T421/S424]. However, this cannot be observed experimentally, since western blot analyses done with a unique anti-phospho-antibody do not discriminate between
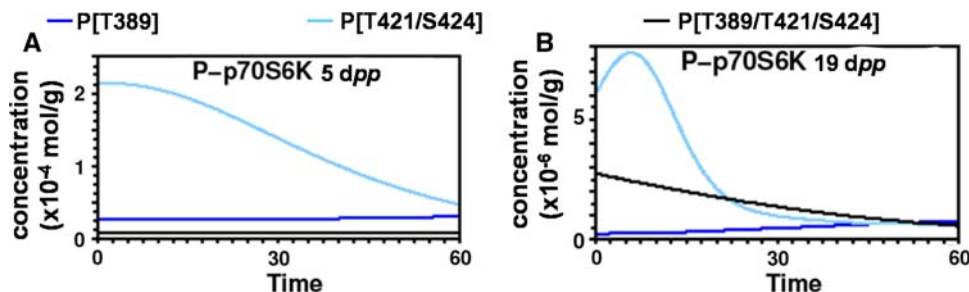
Fig. 10 Simulation of the cAMP/PKA component of FSH-induced p70S6K regulation. Computational simulations (*plain lines*) compared with experimental data (*black crosses* ± SEM) of FSH-R-mediated signaling in the presence of PKA inhibitor, in proliferating (*left*) and differentiating (*right*) Sertoli cells. The concentrations of molecules are expressed as a function of time, as above

regulation by insulin [10], we admit that phosphorylation on the [T389] residue participates in p70S6K activation. Nevertheless, our results indicate that phosphorylation of the [T421/S424] is not a pre-requisite. Therefore, inhibition relief, if any, should be achieved by other aminoacid residues of p70S6K. This view is further supported by the fact that no fit was found unless a supplemental degree of freedom, k7, was added. Presumably, an unidentified effector catalyzes the conversion of p70S6K to p70S6K[T389] in proliferating cells, or, more likely, p70S6K gets phosphorylated at other sites than the two studied here.

Sertoli cells can be considered as a particular cell type. In the neonate, they are differentiating cells which retain some mitotic potential, whereas in the pre-pubertal animal, they lose their mitotic ability and their terminal differentiation is finally acquired in the adult. Interestingly, a single hormone, FSH, is a key regulator of these developmental processes, hence its signaling can be analyzed in two different and physiologically relevant backgrounds. It is now clear that the signaling pathways activated by FSH at each stage of Sertoli cell post-natal development are different, or, at least, differentially modulated to lead to those various cellular responses. For example, in 5-day-old rat proliferating Sertoli cells, the MAP kinases ERK1 and ERK2 are phosphorylated by FSH [32]. ERK phosphorylation induces a cyclin D1 increase which is directly related to the proliferation state of the cells. In contrast, FSH totally switches off the ERK pathway in 19-day-old rat differentiating Sertoli cells. Likewise, we hypothesized that the signaling pathways activated by FSH upstream of the p70S6K might be different at each of those developmental stages and would result in differential phosphorylation patterns. And actually, the signaling pathways induced by FSH to phosphorylate p70S6K seem to be modulated during the post-natal development of Sertoli cells, leading to different phosphorylation patterns, with differential integration of PI3K- and PKA-dependent signaling mechanisms. In addition, T421/S424 dephosphorylation seems

Pp70S6K[T389] and Pp70S6K[T389/T421/S424]. Therefore, although the PIP3 level was not significantly increased following FSH stimulation, we propose that there was still an increase in the phosphorylation of the PIP3-sensitive site, T389. In contrast, in proliferating cells, as a result from conflicting interactions of the PKA- and the PI3K-dependent component, Pp70S6K[T389/T421/S424] is the active form following FSH stimulation. When compared to the admitted model of p70S6K

Fig. 11 Intrinsic Pp70S6K quantities predicted by computational simulations, in PKA-perturbed conditions. As above, the respective levels of Pp70S6K phosphorylated on [T389] only, Pp70S6K

phosphorylated on [T421/S424] only and Pp70S6K phosphorylated on [T389/T421/S424], are compared. Simulations in **a** proliferating and **b** differentiating Sertoli cells are shown

Fig. 12 Graphic representation of the developmental regulation of p70S6K by FSH and by insulin. **a** Regulation of p70S6K by FSH has been superimposed to highlight the differences between both stages. The reactions specifically induced by FSH in proliferating cells are in *green*, while those specifically induced by FSH in differentiating cells are in *red*, and the common ones are in *black*. The active form of p70S6K is surrounded by *green* and *red dots*, respectively. **b** Insulin induces a similar pattern of p70S6K phosphorylation at both stages. The molecular species experimentally measured in this study and mined for the simulations are in color, while the others are in *black* and *white*. All the reactions are equilibrium, but for clarity, they are represented with simple *arrows*, unless necessary. Reaction parameters, as determined by data fitting, are indicated. Activating interactions are figured with a *line* ended in a *circle*
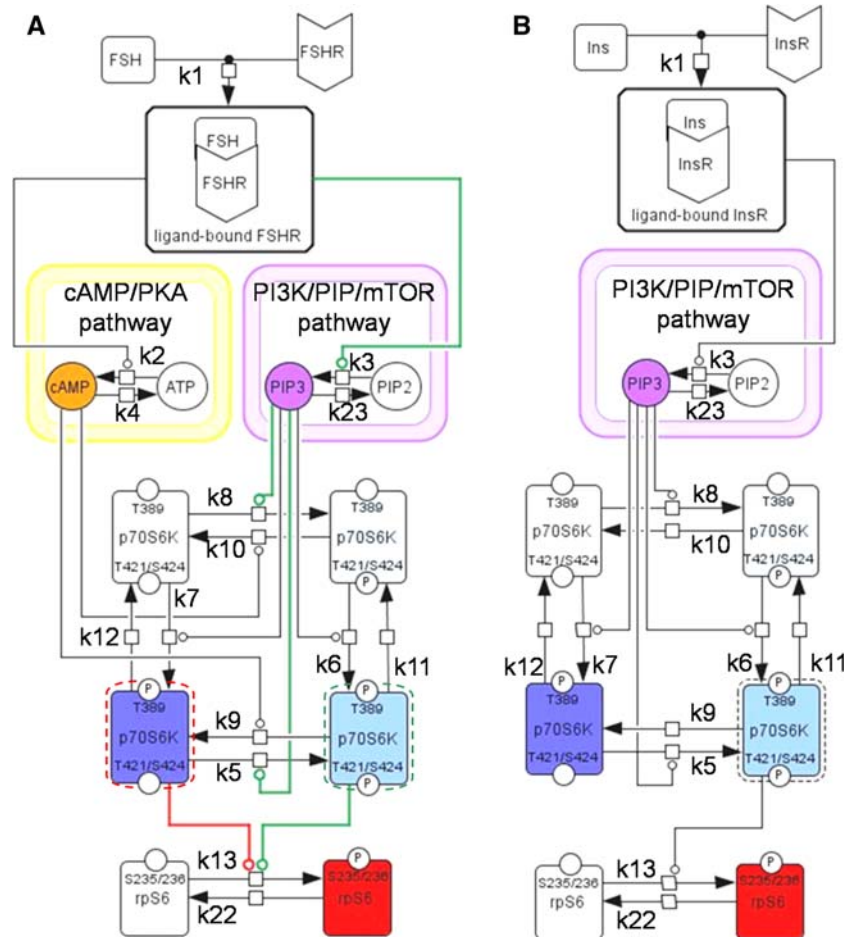
to have different consequences on p70S6K activity in the two stages: activating in differentiating cells and inhibitory in proliferating cells. Therefore, the cellular background appears to be instrumental for p70S6K phosphorylation and activity, in agreement with the notion that the developmental stage of cells dictates the way the hormonal messages are integrated. p70S6K is also activated by FSH in granulosa cells of the ovary, in a PKA-dependent manner, but only phosphorylation on the T389 site has been analyzed in this study [37].

One possibility to explain the developmental regulation of p70S6K by second messenger-dependent kinases was that second messenger production in response to FSH would be developmentally regulated, depending on FSH-R coupling to various G proteins. For this reason, we analyzed the efficacy of FSH to induce PIP3 and cAMP downstream. The cAMP basal level was much higher in proliferating cells than in differentiating cells [32] but the FSH-induced raise in production was much more important in differentiating cells. Conversely, basal PIP3 production was lower in proliferating cells and significantly increased by FSH, when compared to differentiating cells. These observations could explain that the main pathway required

for FSH to stimulate p70S6K in proliferating cells is the PI3K/mTOR pathway, leading to the inducible phosphorylation of p70S6K T389. This is consistent with the proliferating state of the cells and to the well-known role of this pathway in cell growth [38]. In differentiating cells, the main pathway activated by FSH is the PKA pathway, required for the expression of specific markers, such as transferrin [39]. Again, these findings indicate that a single ligand can stimulate diverse intracellular signaling pathways with differential efficacy. The FSH-R has the ability to couple to both Gs and Gi, depending on the developmental stage [32] or the cell type [40]. The nature of the G proteins that the receptor couples to could be critical for signaling to p70S6K activation, since GPCR coupled to Gq, for example, such as the M3-muscarinic [36], PGF2α [19], α1-adrenergic receptor [41], stimulate p70S6K in a PI3K-independent manner, unlike Gi-coupled receptors, such as the LPA [42] or the μ-opioid [43] receptors. Alternatively, a yeast two-hybrid screen has revealed the direct interaction of the FSH-R with a PI3K adaptor, APPL1 [44], in a signalosome including Foxo1 [45]. Unfortunately, the expression pattern of APPL1 in the development of Sertoli cells is not yet available.

We cannot yet appreciate the biological consequences of the differences in p70S6K regulation in Sertoli cell development and in response to a GPCR or to a tyrosine kinase receptor. Since p70S6K has 8 potential phosphorylation sites [46], more studies are needed to better define the p70S6K pattern of phosphorylation in response to each of those receptors and the outcomes on the biological role of p70S6K. And in fact, modeling the entire combinatorial complexity of p70S6K regulation sites in developing Sertoli cells stimulated by FSH is an interesting question to address in future work. In particular, p70S6K is known to be implicated in mRNA translation, by phosphorylating rpS6 [47], and eIF4B [7]. Whether the different active isoforms of p70S6K that we have studied here equally regulate their target proteins within the translational machinery remains to be defined. GPCRs have recently been linked to the control of translation by the discovery that the GPCR scaffolding proteins β-arrestins are involved in protein synthesis by positively regulating Mnk [48]. Hence, whether the FSH-R and the insulin receptor act on the translational machinery in different manners in Sertoli cell development also needs to be addressed in the future.

References

1. Ohanna M, Sobering AK, Lapointe T, Lorenzo L, Praud C, Petroulakis E, Sonenberg N, Kelly PA, Sotiropoulos A, Pende M (2005) Atrophy of S6K1(−/−) skeletal muscle cells reveals distinct mTOR effectors for cell cycle and size control. Nat Cell Biol 7:286–294

2. Pende M, Kozma SC, Jaquet M, Oorschot V, Burcelin R, Le Marchand-Brustel Y, Klumperman J, Thorens B, Thomas G (2000) Hypoinsulinaemia, glucose intolerance and diminished beta-cell size in S6K1-deficient mice. Nature 408:994–997

3. Lane HA, Fernandez A, Lamb NJ, Thomas G (1993) p70S6K function is essential for G1 progression. Nature 363:170–172

4. Blenis J, Erikson RL (1985) Regulation of a ribosomal protein S6 kinase activity by the Rous sarcoma virus transforming protein, serum, or phorbol ester. Proc Natl Acad Sci USA 82:7621–7625

5. Stewart MJ, Thomas G (1994) Mitogenesis and protein synthesis: a role for ribosomal protein S6 phosphorylation? Bioessays 16:809–815

6. Rogers GW Jr, Richter NJ, Merrick WC (1999) Biochemical and kinetic characterization of the RNA helicase activity of eukaryotic initiation factor 4A. J Biol Chem 274:12236–12244

7. Raught B, Peiretti F, Gingras AC, Livingstone M, Shahbazian D, Mayeur GL, Polakiewicz RD, Sonenberg N, Hershey JW (2004) Phosphorylation of eucaryotic translation initiation factor 4B Ser422 is modulated by S6 kinases. EMBO J 23:1761–1769

8. Holz MK, Ballif BA, Gygi SP, Blenis J (2005) mTOR and S6K1 mediate assembly of the translation preinitiation complex through dynamic protein interchange and ordered phosphorylation events. Cell 123:569–580

9. Burnett PE, Barrow RK, Cohen NA, Snyder SH, Sabatini DM (1998) RAFT1 phosphorylation of the translational regulators p70 S6 kinase and 4E-BP1. Proc Natl Acad Sci USA 95:1432–1437

10. Dennis PB, Pullen N, Pearson RB, Kozma SC, Thomas G (1998) Phosphorylation sites in the autoinhibitory domain participate in p70(s6k) activation loop phosphorylation. J Biol Chem 273:14845–14852

11. Pullen N, Thomas G (1997) The modular phosphorylation and activation of p70S6K. FEBS Lett 410:78–82

12. Dennis PB, Pullen N, Kozma SC, Thomas G (1996) The principal rapamycin-sensitive p70(s6 k) phosphorylation sites, T-229 and T-389, are differentially regulated by rapamycin-insensitive kinase kinases. Mol Cell Biol 16:6242–6251

13. Pullen N, Dennis PB, Andjelkovic M, Dufner A, Kozma SC, Hemmings BA, Thomas G (1998) Phosphorylation and activation of p70S6K by PDK1. Science 279:707–710

14. Ma L, Chen Z, Erdjument-Bromage H, Tempst P, Pandolfi PP (2005) Phosphorylation and functional inactivation of TSC2 by Erk implications for tuberous sclerosis and cancer pathogenesis. Cell 121:179–193

15. Proud CG (2007) Signalling to translation: how signal transduction pathways control the protein synthetic machinery. Biochem J 403:217–234

16. Edelmann HM, Kuhne C, Petritsch C, Ballou LM (1996) Cell cycle regulation of p70 S6 kinase and p42/p44 mitogen-activated protein kinases in Swiss mouse 3T3 fibroblasts. J Biol Chem 271:963–971

17. Le XF, Hittelman WN, Liu J, McWatters A, Li C, Mills GB, Bast RC Jr (2003) Paclitaxel induces inactivation of p70 S6 kinase and phosphorylation of Thr421 and Ser424 via multiple signaling pathways in mitosis. Oncogene 22:484–497

18. Suh JM, Song JH, Kim DW, Kim H, Chung HK, Hwang JH, Kim JM, Hwang ES, Chung J, Han JH, Cho BY, Ro HK, Shong M (2003) Regulation of the phosphatidylinositol 3-kinase, Akt/ protein kinase B, FRAP/mammalian target of rapamycin, and ribosomal S6 kinase 1 signaling pathways by thyroid-stimulating hormone (TSH) and stimulating type TSH receptor antibodies in the thyroid gland. J Biol Chem 278:21960–21971

19. Arvisais EW, Romanelli A, Hou X, Davis JS (2006) AKT-independent phosphorylation of TSC2 and activation of mTOR and ribosomal protein S6 kinase signaling by prostaglandin F2alpha. J Biol Chem 281:26904–26913

20. Moschella PC, Rao VU, McDermott PJ, Kuppuswamy D (2007) Regulation of mTOR and S6K1 activation by the nPKC isoforms, PKCepsilon and PKCdelta, in adult cardiac muscle cells. J Mol Cell Cardiol 43:754–766

21. Ballou LM, Cross ME, Huang S, McReynolds EM, Zhang BX, Lin RZ (2000) Differential regulation of the phosphatidylinositol 3-kinase/Akt and p70 S6 kinase pathways by the alpha(1A)-adrenergic receptor in rat-1 fibroblasts. J Biol Chem 275:4803–4809

22. Lecureuil C, Tesseraud S, Kara E, Martinat N, Sow A, Fontaine I, Gauthier C, Reiter E, Guillou F, Crepieux P (2005) Follicle-stimulating hormone activates p70 ribosomal protein S6 kinase

by protein kinase A-mediated dephosphorylation of Thr 421/Ser 424 in primary Sertoli cells. Mol Endocrinol 19:1812–1820

23. Dierich A, Sairam MR, Monaco L, Fimia GM, Gansmuller A, LeMeur M, Sassone-Corsi P (1998) Impairing follicle-stimulating hormone (FSH) signaling in vivo: targeted disruption of the FSH receptor leads to aberrant gametogenesis and hormonal imbalance. Proc Natl Acad Sci USA 95:13612–13617

24. Kumar TR, Wang Y, Lu N, Matzuk MM (1997) Follicle stimulating hormone is required for ovarian follicle maturation but not male fertility. Nat Genet 15:201–204

25. Sairam MR, Krishnamurthy H (2001) The role of follicle-stimulating hormone in spermatogenesis: lessons from knockout animal models. Arch Med Res 32:601–608

26. Wayne CM, Fan HY, Cheng X, Richards JS (2007) Follicle-stimulating hormone induces multiple signaling cascades: evidence that activation of Rous sarcoma oncogene, RAS, and the epidermal growth factor receptor are critical for granulosa cell differentiation. Mol Endocrinol 21:1940–1957

27. Kara E, Crepieux P, Gauthier C, Martinat N, Piketty V, Guillou F, Reiter E (2006) A phosphorylation cluster of five serine and threonine residues in the C-terminus of the follicle-stimulating hormone receptor is important for desensitization but not for beta-arrestin-mediated ERK activation. Mol Endocrinol 20:3014–3026

28. Guillou F, Martinat N, Combarnous Y (1986) Study of the superactivity of equine follicle-stimulating hormone in in vitro stimulation of rat Sertoli cells. Biochem Biophys Acta 887:196–203

29. Bernard L, Martinat N, Lécureuil C, Crépieux P, Reiter E, Tilloy-Ellul A, Chevalier S, Guillou F (2007) Dichlorodiphenyltrichloroethane impairs follicle-stimulating hormone receptor-mediated signaling in rat Sertoli cells. Reprod Toxicol 23:158–164

30. Guillou H, Lecureuil C, Anderson KE, Suire S, Ferguson GJ, Ellson CD, Gray A, Divecha N, Hawkins PT, Stephens LR (2007) Use of the GRP1 PH domain as a tool to measure the relative levels of PtdIns(3, 4, 5)P3 through a protein-lipid overlay approach. J Lipid Res 48:726–732

31. Nishio Y, Nagata S, Umeda M, Shirai R, Yokogawa T, Ihara S, Fukui Y (2000) Quantification of phosphatidylinositol 3, 4, 5-trisphosphate by liposome lysis assay with specific monoclonal antibodies. Anal Biochem 285:270–273

32. Crépieux P, Marion S, Martinat N, Fafeur V, Vern YL, Kerboeuf D, Guillou F, Reiter E (2001) The ERK-dependent signalling is stage-specifically modulated by FSH, during primary Sertoli cell maturation. Oncogene 20:4696–4709

33. Bortolussi M, Zanchetta R, Belvedere P, Colombo L (1990) Sertoli and Leydig cell numbers and gonadotropin receptors in rat testis from birth to puberty. Cell Tissue Res 260:185–191

34. Monn E, Desautel M, Christiansen RO (1972) Highly specific testicular adenosine-3′, 5′-monophosphate phosphodiesterase associated with sexual maturation. Endocrinology 91:716–720

35. Murray AJ (2008) Pharmacological PKA inhibition: all may not be what it seems. Sci Signal 1, re4

36. Tang X, Wang L, Proud CG, Downes CP (2003) Muscarinic receptor-mediated activation of p70 S6 kinase 1 (S6K1) in 1321N1 astrocytoma cells: permissive role of phosphoinositide 3-kinase. Biochem J 374:137–143

37. Alam H, Maizels ET, Park Y, Ghaey S, Feiger ZJ, Chandel NS, Hunzicker-Dunn M (2004) FSH activation of HIF-1 by the PI3-kinase/AKT/Rheb/mTOR pathway is necessary for induction of select protein markers of follicular differentiation. J Biol Chem 279:19431–19440

38. Shaw RJ, Cantley LC (2006) Ras, PI(3)K and mTOR signalling controls tumour cell growth. Nature 441:424–430

39. Suire S, Fontaine I, Guillou F (1995) Follicle stimulating hormone (FSH) stimulates transferrin gene transcription in rat Sertoli cells: cis and trans-acting elements involved in FSH action via cyclic adenosine 3′, 5′-monophosphate on the transferrin gene. Mol Endocrinol 9:756–766

40. Sun L, Peng Y, Sharrow AC, Iqbal J, Zhang Z, Papachristou DJ, Zaidi S, Zhu LL, Yaroslavskiy BB, Zhou H, Zallone A, Sairam MR, Kumar TR, Bo W, Braun J, Cardoso-Landa L, Schaffler MB, Moonga BS, Blair HC, Zaidi M (2006) FSH directly regulates bone mass. Cell 125:247–260

41. Wang L, Proud CG (2002) Ras/Erk signaling is essential for activation of protein synthesis by Gq protein-coupled receptor agonists in adult cardiomyocytes. Circ Res 91:821–829

42. Kam Y, Exton JH (2004) Role of phospholipase D1 in the regulation of mTOR activity by lysophosphatidic acid. FASEB J 18:311–319

43. Polakiewicz RD, Schieferl SM, Gingras AC, Sonenberg N, Comb MJ (1998) mu-Opioid receptor activates signaling pathways implicated in cell survival and translational control. J Biol Chem 273:23534–23541

44. Nechamen CA, Thomas RM, Cohen BD, Acevedo G, Poulikakos PI, Testa JR, Dias JA (2004) Human follicle-stimulating hormone (FSH) receptor interacts with the adaptor protein APPL1 in HEK 293 cells: potential involvement of the PI3K pathway in FSH signaling. Biol Reprod 71:629–636

45. Nechamen CA, Thomas RM, Dias JA (2007) APPL1, APPL2, Akt2 and FOXO1a interact with FSHR in a potential signaling complex. Mol Cell Endocrinol 260–262:93–99

46. Ferrari S, Bannwarth W, Morley SJ, Totty NF, Thomas G (1992) Activation of p70S6K is associated with phosphorylation of four clustered sites displaying Ser/Thr-Pro motifs. Proc Natl Acad Sci USA 89:7282–7286

47. Duncan R, McConkey EH (1982) Rapid alterations in initiation rate and recruitment of inactive RNA are temporally correlated with S6 phosphorylation. Eur J Biochem 123:539–544

48. DeWire SM, Kim J, Whalen EJ, Ahn S, Chen M, Lefkowitz RJ (2008) Beta-arrestin-mediated signaling regulates protein synthesis. J Biol Chem 283:10611–10620